

SPATIAL GROUND MOTION EFFECT ON RELATIVE DISPLACEMENT OF ADJACENT BUILDING STRUCTURES

HONG HAO^{1,*†} AND SE-RONG ZHANG^{2,‡}

¹*School of Civil and Structural Engineering, Nanyang Technological University, Singapore 639798, Singapore*

²*Department of Hydraulic and Harbor Engineering, Tianjin University, Tianjin 300072, People's Republic of China*

SUMMARY

This paper analyses earthquake ground motion spatial variation effects on relative linear elastic response of adjacent building structures. It studies the relative importance of ground motion spatial variations and dynamic characteristics of adjacent structures in causing relative responses. Random vibration method is used in the study. It is found that, besides ground-acceleration-induced dynamic responses, quasi-static responses induced by spatially varying ground displacements also contribute significantly to the relative structural responses. The effects of spatial ground motions are very pronounced to the relative displacements of adjacent low-rise structures, and to those of high-rise adjacent structures with similar vibration characteristics. The effect of vibration properties of adjacent structures are, however, more significant to those of high-rise adjacent structures if they poses noticeably different vibration periods. Copyright © 1999 John Wiley & Sons, Ltd.

KEY WORDS: spatial ground motion; quasi-static displacement; dynamic displacement; relative response; pounding

INTRODUCTION

Seismic pounding damage to inadequately separated adjacent building structures has been reported in the last 30 years in almost all the major earthquakes. For example, a large number of adjacent buildings were severely damaged and partially collapsed during the 1985 Mexico earthquake. Analysis of damage statistics revealed first that pounding between adjacent buildings occurred in over 40 per cent of the 330 collapsed or severely damaged buildings, and for at least 15 per cent of them, pounding was the primary cause for collapse.¹ Although it was subsequently pointed out that the reported number of pounding damage in Mexico City during the 1985 earthquake might be an overestimation,² the event has surely attracted more concerns on pounding damage to adjacent structures during strong earthquakes. Field investigation was carried out after the 1989 Loma Prieta earthquake in California,³ it was reported that more than 200 cases of pounding were observed in the 500 buildings surveyed; architectural damage was found in over 79 per cent of them, while 21 per cent of the same buildings endured significant

* Correspondence to: Hong Hao, School of Civil and Structural Engineering, Nanyang Technological University, Blk N1, # 1A-37, Nanyang Avenue, Singapore 639798. E-mail: chhao@ntu.edu.sg

† Senior Lecturer

‡ Associate Professor

structural destruction. Not surprisingly, pounding damage was also observed after the 1988 Sequenay earthquake in Canada, the 1992 Erzincan earthquake in Turkey, the 1992 Cairo earthquake, and the 1995 Kobe earthquake. An excellent review of the reported pounding damage was given by Anagnostopoulos.⁴

Due to the difference in dynamic properties and spatially varying ground excitations, adjacent structures will experience out-of-phase responses during a strong earthquake. If initial separation between them is not adequate, pounding will occur. Studies of seismic pounding effects have been conducted by many researchers.^{5–10} Various pounding mitigation methods have also been suggested, such as filling the gaps, connecting the adjacent structures, using bumper walls, or providing adequate separation to avoid pounding. The most simplest and effective way is to provide enough separation although it is sometimes difficult to be implemented due to detailing problem and high cost of land.

Almost all the major seismic codes such as the Uniform Building Code (UBC),¹¹ National Building Code of Canada (NBCC),¹² Chinese Seismic Building Code (GBJ11-89),¹³ and many others specify a minimum required separation between adjacent structures to avoid pounding. The method to determine the required separation, however, varies from code to code. For example, NBCC and UBC determine the minimum separation based on the sum of the maximum displacements of two adjacent structures, whereas GBJ11-89 specifies the required separation according to the building heights and seismic intensity. It should be noted that code specifications on one hand might overestimate the required separations of high-rise adjacent buildings since they neglect the response phase difference of adjacent structures. On the other hand, they might underestimate the required separations of low-rise structures because they do not take ground motion spatial variation effects into consideration. It is known that spatially varying ground motions induce quasi-static responses that might dominate the overall structural responses of stiff structures.^{14–16}

Many authors estimated the required separations by using time history or random vibration method. In those studies, structures were idealized as either Single-Degree-of-Freedom (SDOF) oscillators^{6,17–20} or multiple-degrees-of-freedom frames.^{7,9} Recently, a spectral difference method was proposed by Jeng *et al.*¹⁸ By simplifying the adjacent structures as two SDOF oscillators with linear elastic properties, the latter study estimated the required separation by using random vibration method. The response phase difference between two structures is accounted for by introducing a correlation coefficient. The method was then extended to include the ground motion wave passage effect¹⁹ and inelastic responses.²⁰ Based on equivalent linearization of non-linear hysteretic behaviour and application of CQC method, an analytical procedure was also suggested to estimate the required separation of adjacent buildings according to the design response spectrum and fundamental periods of two buildings.²¹ Using Tajimi–Kanai²² ground acceleration power spectral density function to model earthquake ground motion, random vibration method is also employed to estimate the required separation between MDOF frame buildings.²³ It should be noted that all the previous studies did not rigorously include ground motion spatial variation effects into consideration although the work by Jeng and Kasai¹⁹ considered wave passage effects.

In the present paper, parametric study is carried out to investigate the effects of ground motion spatial variations and structural vibration characteristics on relative displacement of adjacent buildings. Random vibration method is employed in the study. Linear elastic responses of adjacent reinforced concrete moment resistant frames are considered. Ground motion is modeled by a filtered Tajimi–Kanai power spectral density function²⁴ together with an empirical

Table I. Column size and reinforcement ratio

Storey number	1-storey (Steel ratio)	2-storey (Steel ratio)	20-storey (Steel ratio)	24-storey (Steel ratio)
21–24				250 × 400 (2)
16–20			250 × 400 (2)	250 × 500 (4)
10–15			250 × 500 (4)	250 × 700 (4)
7–9			250 × 700 (4)	250 × 800 (5)
4–6			250 × 800 (6)	250 × 1000 (6)
1–3	250 × 400 (2)	250 × 400 (2)	250 × 1000 (6)	250 × 1100 (6)

coherency function.²⁵ Numerical results are presented in terms of dimensionless parameters. The effects of various ground motion spatial variation characteristics and structural vibration properties on relative displacement are discussed.

MOMENT-RESISTANT RC FRAMES

Four realistic moment-resistant RC frames, namely an 1-storey, a 2-storey, a 20-storey and a 24-storey RC frames, are considered. The first-storey height is 3.5 m and the rest 3.0 m for the four frames. All the beams are assumed having a cross-sectional area of $230 \times 300 \text{ mm}^2$ and a reinforcement ratio of 2 per cent. The dimensions and reinforcement ratios of columns are given in Table I. The span length d is assumed to be 10 m if it is not otherwise mentioned in numerical calculation. The lumped mass at each floor level is calculated by using the unit weight of 24 kN/m^3 for RC structures. The damping ratios for all the vibration modes are assumed to be 5 per cent in numerical calculation.

Relative displacement is defined as the displacement difference between those at the roofs of two same height buildings, or roof of the lower building and the corresponding floor of the higher one if two adjacent structures do not have the same height. Those between the two 2-storey buildings, the two 24-storey buildings, the 1-storey and the 2-storey buildings, and the 20-storey and the 24-storey buildings are calculated. In numerical calculation, ground excitations at the adjacent supports of two buildings are assumed to be the same, thus there are three spatially varying ground displacements v_{g1} , v_{g2} , and v_{g3} as shown in Figure 1.

SPATIAL GROUND MOTIONS

Cross power spectral density function of spatial ground motions at points i and j on ground surface can be written as

$$S_{ij}(i\bar{\omega}) = S_g(\bar{\omega})\gamma_{ij}(i\bar{\omega}, d_{ij}) \quad (1)$$

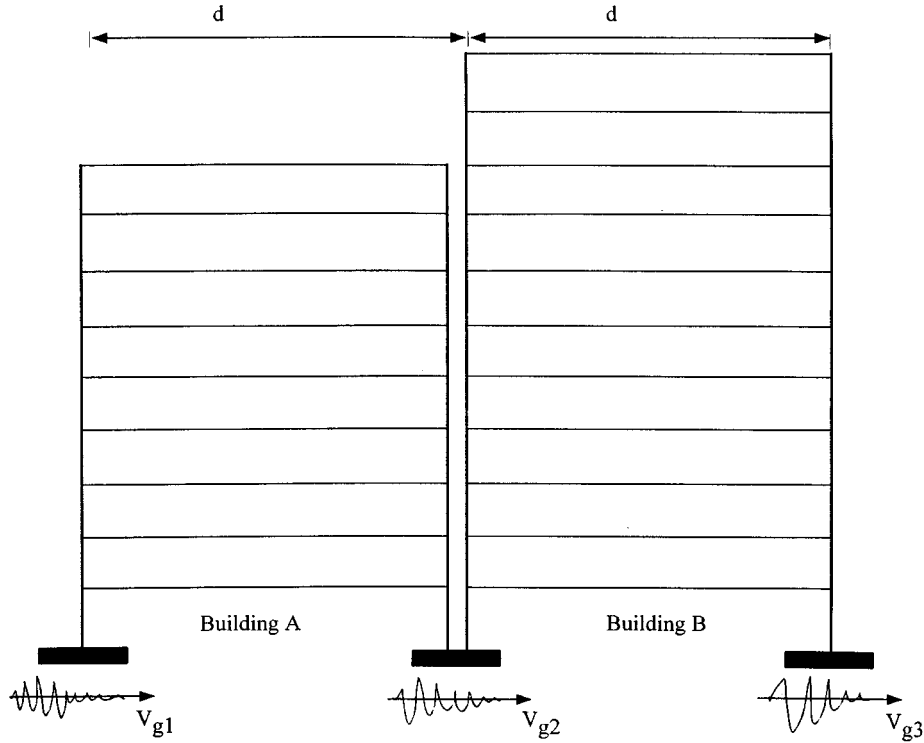


Figure 1. Adjacent RC frame buildings subjected to spatially varying ground excitations (not to scale)

where

$$S_g(\bar{\omega}) = |H_p(\bar{\omega})|^2 S_o(\bar{\omega}) = \frac{\bar{\omega}^4}{(\omega_p^2 - \bar{\omega}^2)^2 + 4\xi_p^2 \omega_p^2 \bar{\omega}^2} \frac{1 + 4\xi_g^2 \bar{\omega}^2 / \omega_g^2}{(1 - \bar{\omega}^2 / \omega_g^2)^2 + 4\xi_g^2 \bar{\omega}^2 / \omega_g^2} \Gamma \quad (2)$$

is a filtered Tajimi–Kanai power spectral density function,²⁴ in which $|H_p(\bar{\omega})|^2$ is a high pass filter, $S_o(\bar{\omega})$ is the Tajimi–Kanai power spectral density function, $\bar{\omega}$ is circular frequency, ω_p and ξ_p are central frequency and damping ratio of the high pass filter, ω_g and ξ_g are central frequency and damping ratio of the Tajimi–Kanai power spectral density function, and Γ depending on ground motion intensity is a scaling factor.

$$\gamma_{ij}(i\bar{\omega}, d_{ij}) = |\gamma_{ij}(i\bar{\omega}, d_{ij})| e^{-i\bar{\omega} d_{ij}/v} \quad (3)$$

is an empirical coherency function,²⁵ where

$$|\gamma_{ij}(i\bar{\omega}, d_{ij})| = \exp(-\beta d_{ij}) \exp \left[-\alpha(\bar{\omega}) \sqrt{d_{ij}} \left(\frac{\bar{\omega}}{2\pi} \right)^2 \right] \quad (4)$$

in which d_{ij} is the projected distance in the wave propagation direction between points i and j on ground surface, β is a constant and $\alpha(\bar{\omega})$ is a function with the form

$$\alpha(\bar{\omega}) = a \frac{\bar{\omega}}{2\pi} + b \frac{2\pi}{\bar{\omega}} + c \quad (5)$$

The constants a , b , c and β can be obtained by least-squares fitting the coherency function of recorded motions.

In the present study, the central frequency $\omega_g = 5\pi$ rad/s and $\xi_g = 0.6$ are used, which correspond to those of a typical hard soil site. The scale factor $\Gamma = 0.044 \text{ m}^2/\text{s}^3$, which corresponds to a ground acceleration with a duration of 20 s and a Peak Value (PGA) of 0.5 g .²⁶ The constants in coherency function are $a = 35.83 \times 10^{-4}$, $b = -0.181 \times 10^{-4}$, $c = 1.177 \times 10^{-4}$, and $\beta = 1.109$, which were obtained by processing recorded motions during event 45 at the SMART-1 array;²⁵ an apparent velocity of $v = 1000 \text{ m/s}$ is assumed in most numerical calculations if it is not specifically mentioned.

Ground displacement power spectral density function can be derived as

$$S_d(\bar{\omega}) = \frac{1}{\bar{\omega}^4} S_g(\bar{\omega}) \quad (6)$$

It is known that varying the central frequency of high pass filter, ω_p , will not affect ground acceleration noticeably, but it will change ground displacement significantly. Using a smaller ω_p will result in a larger ground displacement. Using the random vibration method presented in Appendix I and ground displacement power spectral density function, peak ground displacements are calculated. Figure 2 shows the computed peak ground displacements as a function of Γ obtained with $\xi_p = 0.6$ and different ω_p .

The high pass filter $|H_p(\bar{\omega})|^2$ is used to filter out ground acceleration energy at very low frequencies to eliminate drifting of ground velocity and displacement. It is only a mathematical filter without any solid physical meaning. Using this high pass filter generally yields satisfactory results if ground excitations are assumed to be uniform since it has little effect on ground

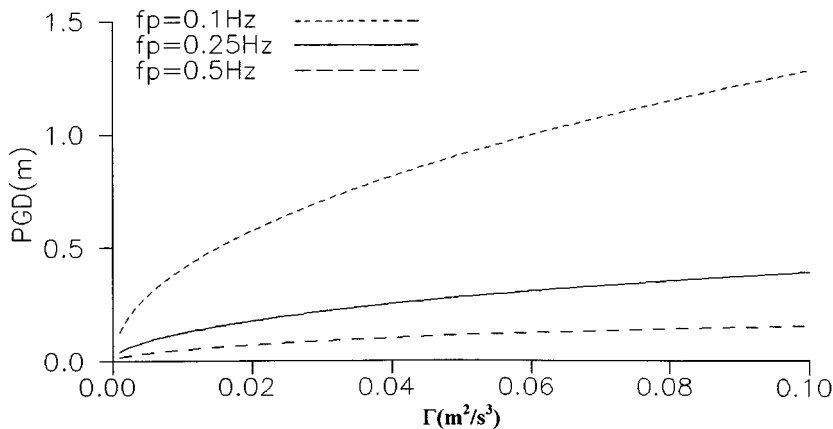


Figure 2. Peak ground displacement with respect to different ground motion intensities

acceleration. When studying structural response to spatially varying ground excitations, spatial ground displacements cause quasi-static responses. Thus, an appropriate high pass filter becomes very important because it affects ground displacement significantly. In the present study, however, the commonly used high pass filter defined by Ruiz and Penzien²⁴ is still employed, but different values of ω_p , namely $f_p = \omega_p/2\pi = 0.1, 0.25$ and 0.5 Hz, are used to study its effect on structural responses.

Since ground displacement cannot be recorded, current practice double integrates recorded ground acceleration to obtain ground displacement. The high pass filter has to be applied to ground acceleration to eliminate drifting of ground velocity and displacement. It is a great challenge to determine the exact value of ω_p since no actually recorded ground displacement is available. ω_p is believed depending on the epicentral distance, path effect, and local site effect. Generally speaking, a smaller ω_p should be used if epicentral distance is longer and local site is softer.

EQUATION FORMULATION

By lumping the storey mass of a frame building to its respective floors, the dynamic equilibrium equation in matrix form can be written as

$$\begin{bmatrix} \mathbf{m}_{ss} & \mathbf{0} \\ \mathbf{0} & \mathbf{0} \end{bmatrix} \begin{Bmatrix} \ddot{\mathbf{y}} \\ \ddot{\mathbf{v}}_g \end{Bmatrix} + \begin{bmatrix} \mathbf{c}_{ss} & \mathbf{0} \\ \mathbf{0} & \mathbf{0} \end{bmatrix} \begin{Bmatrix} \dot{\mathbf{y}} \\ \dot{\mathbf{v}}_g \end{Bmatrix} + \begin{bmatrix} \mathbf{k}_{ss} & \mathbf{k}_{sb} \\ \mathbf{k}_{sb}^T & \mathbf{k}_{bb} \end{bmatrix} \begin{Bmatrix} \mathbf{y} \\ \mathbf{v}_g \end{Bmatrix} = \begin{Bmatrix} \mathbf{0} \\ \mathbf{0} \end{Bmatrix} \quad (7)$$

where \mathbf{m}_{ss} is a diagonal lumped mass matrix, \mathbf{c}_{ss} is a viscous damping matrix, \mathbf{k}_{ss} is a stiffness matrix corresponding to the structural degrees of freedom, \mathbf{k}_{sb} is a coupled stiffness matrix between the structural degrees of freedom and the base movements, \mathbf{k}_{bb} is that corresponding to the base movements, \mathbf{y} is a vector of structural responses, \mathbf{v}_g is a vector of ground displacements at structural supports. In the present study, $\mathbf{v}_g^T = \{v_{g1}, v_{g2}, v_{g3}\}$ as shown in Figure 1, and in which the superscript 'T' represents a matrix transpose.

The structural response equation is

$$\mathbf{m}_{ss}\ddot{\mathbf{y}} + \mathbf{c}_{ss}\dot{\mathbf{y}} + \mathbf{k}_{ss}\mathbf{y} = -\mathbf{k}_{sb}\mathbf{v}_g \quad (8)$$

Equation (8) can be decoupled into its modal vibration equation as

$$\ddot{q}_i + 2\xi_i\omega_i\dot{q}_i + \omega_i^2q_i = -\frac{\varphi_i^T\mathbf{k}_{sb}}{\varphi_i^T\mathbf{m}_{ss}\varphi_i}\mathbf{v}_g \quad (9)$$

where φ_i is the i th vibration mode shape of the structure, q_i is the i th modal response, ω_i and ξ_i are the corresponding circular frequency and viscous damping ratio, respectively.

The structural response at the k th degree of freedom is

$$y^k(t) = \sum_{i=1}^m \varphi_i^k q_i \quad (10)$$

where m is the number of modes considered in the calculation, and φ_i^k is the mode shape value corresponding to the k th degree of freedom.

Using super- or subscripts 'A' and 'B' to denote buildings A and B, respectively, the relative displacement between the k th degree of freedom of building A and the l th degree of freedom of building B is then

$$y_{\text{rel}}(t) = y_A^k(t) - y_B^l(t) = \sum_{i=1}^{m_A} \varphi_{Ai}^k q_{Ai}(t) - \sum_{j=1}^{m_B} \varphi_{Bj}^l q_{Bj}(t) \quad (11)$$

Transfer equation (11) into the frequency domain, it has

$$\bar{y}_{\text{rel}}(\bar{\omega}) = \sum_{i=1}^{m_A} \varphi_{Ai}^k \bar{q}_{Ai}(i\bar{\omega}) - \sum_{j=1}^{m_B} \varphi_{Bj}^l \bar{q}_{Bj}(i\bar{\omega}) \quad (12)$$

The i th modal response of building A can be obtained from equation (9) as

$$\bar{q}_{Ai}(i\bar{\omega}) = H_{Ai}(i\bar{\omega}) \sum_{r=1}^{n_A} \psi_{ri}^A \bar{v}_{gr}(i\bar{\omega}) \quad (13)$$

in which n_A is the total number of supports of building A, and

$$\psi_{ri}^A = -\frac{\varphi_{Ai}^T \mathbf{k}_{sb}^{Ar}}{\varphi_{Ai}^T \mathbf{m}_{ss}^A \varphi_{Ai}} \quad (14)$$

is the quasi-static participation coefficient for the i th mode corresponding to a movement at support r , \mathbf{k}_{sb}^{Ar} is a vector in coupled stiffness matrix \mathbf{k}_{sb}^A corresponding to support r of building A, and

$$H_{Ai}(i\bar{\omega}) = \frac{1}{(\bar{\omega}^2 - \omega_{Ai}^2) + 2i\zeta_{Ai}\bar{\omega}\omega_{Ai}} \quad (15)$$

is the i th mode frequency transfer function.

Substituting equation (13) into equation (12), the power spectral density function of relative displacement can be derived as

$$S_{y_{\text{rel}}}(\bar{\omega}) = S_{y_A^k}(\bar{\omega}) + S_{y_B^l}(\bar{\omega}) - 2 \operatorname{Re}[S_{y_A^k y_B^l}(i\bar{\omega})] \quad (16)$$

where 'Re' indicates the real part of a complex number.

In the present study, only shear-beam-type buildings with two column lines are considered. If the two columns of each building model are the same, the quasi-static participation coefficients due to ground movements at supports r and s will be the same, that is $\psi_{ri}^A = \psi_{si}^A$. Thus, let the two supports of building A be supports 1 and 2, those of building B be supports 2 and 3, it has

$$S_{y_A^k}(\bar{\omega}) = \frac{2}{\bar{\omega}^4} \left[\sum_{i=1}^{m_A} \sum_{j=1}^{m_A} \varphi_{Ai}^k \varphi_{Aj}^k H_{Ai}(i\bar{\omega}) H_{Aj}^*(i\bar{\omega}) \sum_{r=1}^{n_A} \sum_{s=1}^{n_A} \psi_{ri}^A \psi_{sj}^A \right] \left(1 + |\gamma_{12}| \cos \frac{\bar{\omega} d_{12}}{v} \right) S_g(\bar{\omega}) \quad (17)$$

$$S_{y_B^l}(\bar{\omega}) = \frac{2}{\bar{\omega}^4} \left[\sum_{i=1}^{m_B} \sum_{j=1}^{m_B} \varphi_{Bi}^l \varphi_{Bj}^l H_{Bi}(i\bar{\omega}) H_{Bj}^*(i\bar{\omega}) \sum_{r=1}^{n_B} \sum_{s=1}^{n_B} \psi_{ri}^B \psi_{sj}^B \right] \left(1 + |\gamma_{23}| \cos \frac{\bar{\omega} d_{23}}{v} \right) S_g(\bar{\omega}) \quad (18)$$

and

$$S_{y_A^k y_B^l}(i\bar{\omega}) = \frac{1}{\bar{\omega}^4} \left[\sum_{i=1}^{m_A} \sum_{j=1}^{m_B} \varphi_{Ai}^k \varphi_{Bj}^l H_{Ai}(i\bar{\omega}) H_{Bj}^*(i\bar{\omega}) \sum_{r=1}^{n_A} \sum_{s=1}^{n_B} \psi_{ri}^A \psi_{sj}^B \right] \times (1 + \gamma_{12} + \gamma_{13} + \gamma_{23}) S_g(\bar{\omega}) \quad (19)$$

where the superscript “*” represents complex conjugate of a complex number. The maximum relative displacement of two adjacent buildings can be computed by using the above power spectral density functions and the random vibration method presented in Appendix I.

QUASI-STATIC RELATIVE DISPLACEMENT

It should be noted that relative displacement calculated by using equation (16) consists of dynamic and quasi-static responses, that is

$$\mathbf{y} = \mathbf{y}^d + \mathbf{y}^{qs} \quad (20)$$

and

$$\mathbf{y}^{qs} = -\mathbf{k}_{ss}^{-1} \mathbf{k}_{sb} \mathbf{v}_g \quad (21)$$

Hence, equation (11) can be rewritten as

$$y_{\text{rel}}(t) = y_A^{kd}(t) - y_B^{ld}(t) + y_A^{kqs}(t) - y_B^{lqs}(t) = y_{\text{rel}}^d(t) + y_{\text{rel}}^{qs}(t) \quad (22)$$

For a n -storey frame building shown in Figure 1, if the i th storey stiffness is k_i , the stiffness matrices can be written as

$$\mathbf{k}_{ss} = \begin{bmatrix} k_n & -k_n & 0 & \cdots & & & & \\ -k_n & k_n + k_{n-1} & -k_{n-1} & \cdots & & & & \\ \vdots & \vdots & \vdots & \cdots & \vdots & \vdots & \vdots & \\ & & & \cdots & -k_i & k_i + k_{i-1} & -k_{i-1} & \cdots \\ & & & & \vdots & \vdots & \vdots & \vdots \\ & & & & & & \cdots & -k_2 & k_2 + k_1 \end{bmatrix} \quad (23)$$

and

$$\mathbf{k}_{sb} = \begin{bmatrix} 0 & 0 \\ 0 & 0 \\ \vdots & \vdots \\ -\frac{k_1}{2} & -\frac{k_1}{2} \end{bmatrix} \quad (24)$$

It can be derived that

$$-\mathbf{k}_{ss}^{-1}\mathbf{k}_{sb} = \begin{bmatrix} \frac{1}{2} & \frac{1}{2} \\ \frac{1}{2} & \frac{1}{2} \\ \vdots & \vdots \\ \frac{1}{2} & \frac{1}{2} \end{bmatrix} \quad (25)$$

Equation (25) indicates that the quasi-static responses of all the degrees of freedom are the same, and they depend on ground displacements only.

The relative quasi-static displacement is thus

$$y_{rel}^{qs}(t) = \frac{1}{2}[v_{g1}(t) + v_{g2}(t)] - \frac{1}{2}[v_{g2}(t) + v_{g3}(t)] = \frac{1}{2}[v_{g1}(t) - v_{g3}(t)] \quad (26)$$

and its power spectral density function can be derived as

$$S_{y_{rel}^{qs}}(\bar{\omega}) = \frac{1}{2\bar{\omega}^4} \left(1 - |\gamma_{13}| \cos \frac{\bar{\omega}d_{13}}{v} \right) S_g(\bar{\omega}) \quad (27)$$

Using the random vibration method presented in Appendix I, peak values of relative quasi-static displacement are calculated. Figure 3 shows the computed results as a function of the scale factor Γ and as a function of distance d_{13} . As can be seen, peak quasi-static relative displacement is almost inversely proportional to the decrease of central frequency of the high pass filter. When $\Gamma = 0.044 \text{ m}^2/\text{s}^3$ (PGA = 0.5 g), it is 0.012, 0.024 and 0.061 m, respectively, when $f_p = \omega_p/2\pi = 0.5, 0.25$ and 0.1 Hz. Peak quasi-static relative displacements corresponding to $f_p = 0.25$ Hz and $v = 500 \text{ m/s}$ are also shown in Figure 3. Slightly larger relative quasi-static displacements are obtained as compared to those with $v = 1000 \text{ m/s}$ because a smaller apparent velocity results in a more significant ground motion phase shift.

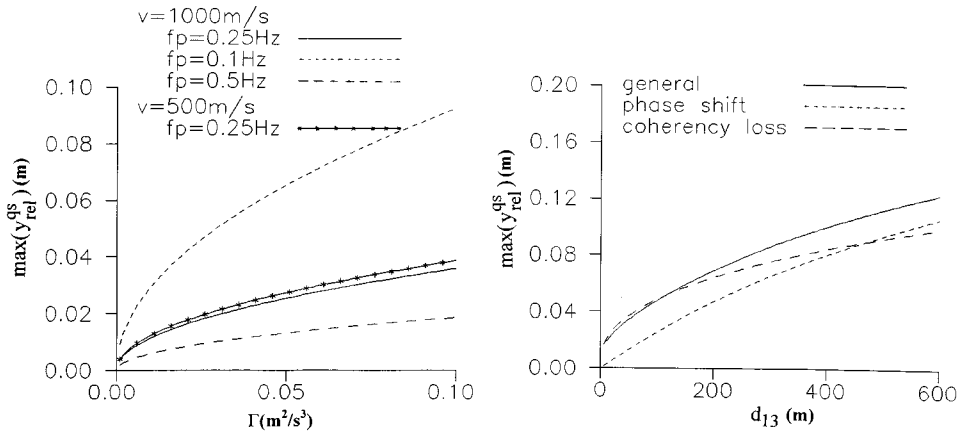


Figure 3. Peak relative quasi-static displacement with respect to different ground motion intensities and different span lengths

Using $f_p = 0.25$ Hz, $v = 1000$ m/s and varying d_{13} , relative quasi-static displacements corresponding to $\text{PGA} = 0.5$ g are also calculated by considering only spatial ground motion variation phase shift ($\gamma_{ij} = \exp(-i\omega d_{ij}/v)$), or only coherency loss ($\gamma_{ij} = |\gamma_{ij}|$). Numerical results are also shown in Figure 3. As can be seen, when $d_{13} = 200$ m, ground motion coherency loss effect is more significant than the phase shift effect. However, as distance d_{13} is longer than 500 m, ground motion phase shift effect becomes more important.

NUMERICAL RESULTS AND DISCUSSION

Using computer program CAL91,²⁷ the vibration frequencies, mode shapes and quasi-static participation coefficients of the four structural models are calculated. Table II lists the first 10 (for 20- and 24-storey structures) modal vibration frequencies and their corresponding quasi-static participation coefficients.

Figure 4 shows the calculated peak relative displacements between two adjacent 24-storey structures, where the first structural model is that presented above and the second one has the same configuration but having continuously and proportionally varying mass along the structural height. Numerical results are presented with respect to the ratio of natural vibration periods of two structures. As can be seen, relative displacement between two structures generally increases as the second structure becomes more and more flexible. When the vibration periods of two structures are close to each other, relative displacement drops rapidly, however, it is not zero at $T_2/T_1 = 1.0$ due to spatially varying ground excitations. Effect of central frequency of the high pass filter is not significant when the second structure is relatively stiff, but it becomes very pronounced when the second structure becomes relatively flexible. These observations indicate that responses are primarily dynamic responses since they are not sensitive to ground displacement, thus not sensitive to f_p . The reason that a high central frequency f_p results in a smaller relative displacement, especially when the second structure is relatively flexible, is because a high central frequency will filter out ground motion energy at low frequencies.

Relative displacement between the 20-storey and the 24-storey structures with mass of the 20-storey structure proportionally varying is also shown in Figure 4. As can be seen, the relative

Table II. Vibration frequencies and quasi-static participation coefficients

Mode i	1-storey		2-storey		20-storey		24-storey	
	f_i (Hz)	$\psi_{ri} = \psi_{si}$	f_i (Hz)	$\psi_{ri} = \psi_{si}$	f_i (Hz)	$\psi_{ri} = \psi_{si}$	f_i (Hz)	$\psi_{ri} = \psi_{si}$
1	6.84	-42754	5.48	-46423	0.520	2574	0.499	-2482
2			15.92	55559	1.41	7936	1.33	8119
3					2.37	13620	2.20	15941
4					3.20	20954	2.93	21667
5					4.08	-22033	3.80	27005
6					4.94	-29410	4.51	32716
7					5.74	29719	5.32	34740
8					6.57	-41622	6.00	34456
9					7.18	-42516	6.81	-33861
10					7.90	39648	7.45	49518

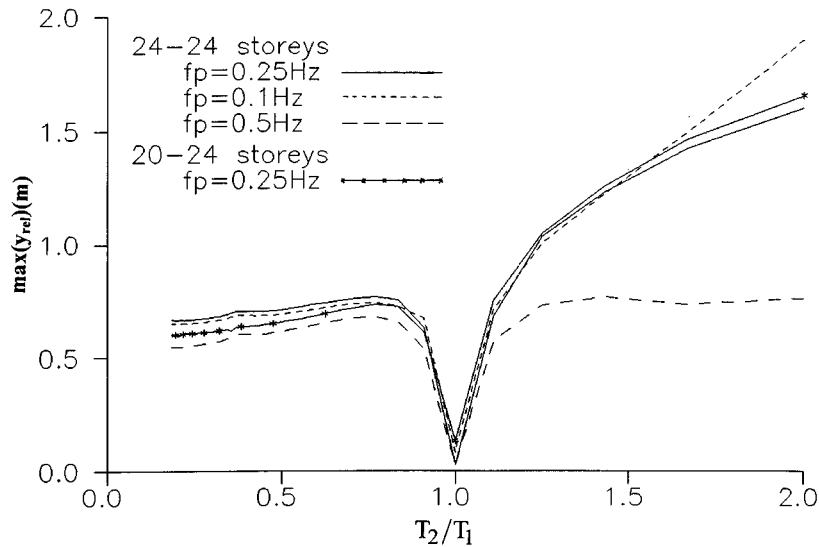


Figure 4. Peak relative displacement calculated with different central frequencies of high pass filter f_p

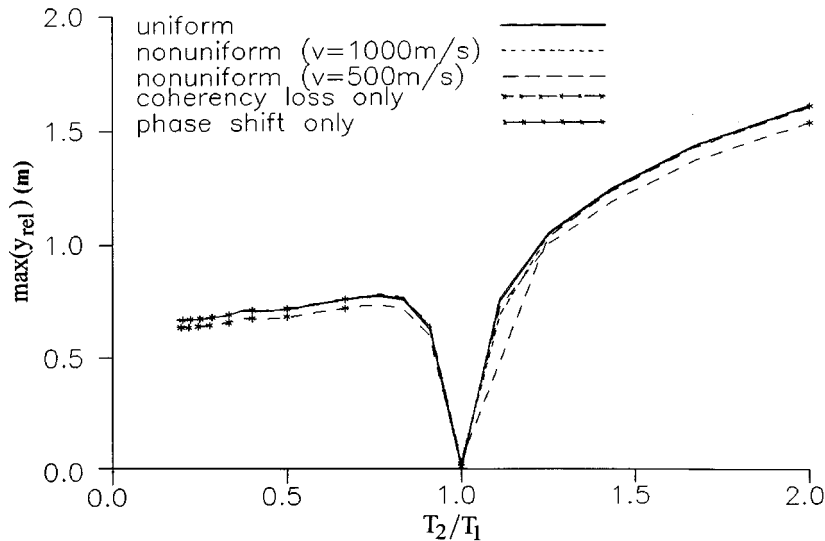


Figure 5. Peak relative displacement calculated with different ground motion spatial variations

displacement is slightly smaller than that between the two 24-storey structures when T_2 (20-storey frame) is less than T_1 . However, it is slightly larger when T_2 is larger than T_1 . This observation implies that the effect of different heights of adjacent high-rise structures is not as important as that of different vibration periods when the height ratio of two adjacent structures is 0.83 (height of 20-storey frame to height of 24-storey frame).

Figure 5 shows the relative displacement between the two 24-storey structures obtained by using multiple ground motions with different spatial variations. As can be seen, the effect of ground motion spatial variation is generally less important than that of different structural vibration properties. Relative displacement is mainly induced because of out-of-phase vibrations between adjacent structures due to their different vibration periods. When the vibration periods of two adjacent structures are close to each other, however, ground motion spatial variation effects become pronounced. The relative displacement is not zero at $T_2/T_1 = 1.0$ when both structures are subjected to non-uniform ground excitations.

Using $v = 500$ m/s, $\text{PGA} = 0.5$ g, $f_p = 0.25$ Hz, and continuously varying the span length d (but keeping the structural vibration frequencies unchanged), relative displacement between the 20- and 24-storey structures ($T_2/T_1 = 1.04$) are calculated by using different spatial ground excitations. Figure 6 shows the numerical results with respect to a dimensionless parameter fd/v , where f is fundamental frequency of the 24-storey structure. The parameter fd/v measures the relation between ground motion phase shift over a distance d and the fundamental vibration mode of the structure with frequency f . $fd/v = 1, 2, \dots$ implies the multiple ground excitations and the fundamental vibration mode are in-phase, whereas they are out-of-phase when $fd/v = 0.5, 1.5, \dots$. It should be noted that $fd/v = 0 - 1.0$ covers most realistic building structures and spatial ground motion velocities. This is because the fundamental frequency of a RC building can be estimated by $f \approx 50/h$, where h is the building's height in meters. It follows that $fd/v = 50d/vh = 50/v\eta$, in which $\eta = h/d$ is the slenderness ratio of the building. It is easy to see that for any combinations of credible values of v and η , the parameter $fd/v = 50/v\eta$ falls indeed in 0.0 and 1.0.

As can be seen, the maximum relative displacement is a constant (about 0.33 m) if structures are subjected to uniform excitation. It increases with fd/v if only spatial ground motion coherency

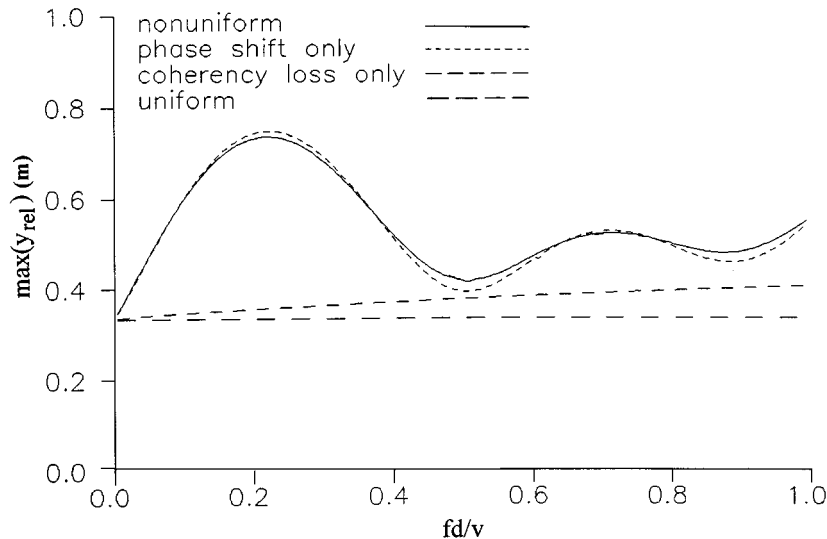


Figure 6. Peak relative displacement between 20- and 24-storey structures obtained with different span lengths and ground motion spatial variations

loss effect is considered, implying coherency loss effect is more significant if either structure is stiffer or span length d is larger. It oscillates with $f d/v$ if ground motion phase shift effect is included. The oscillation reaches the maximum values at $f d/v \approx 0.25, 0.75$ ($f 2d/v \approx 0.5, 1.5$); and the minimum values at $f d/v \approx 0.5, 1.0$ ($f 2d/v \approx 1.0, 2.0$). This implies the largest relative displacement will be produced when the phase shift of spatial ground motions at supports 1 and 3 (separation distance $2d$) are out-of-phase with the fundamental structural vibration mode, whereas the smallest relative displacement will be generated if they are in-phase. The maximum and minimum values do not occur exactly at $f 2d/v = 0.5, 1.5$ or $1.0, 2.0$ because the fundamental vibration frequency of 20-storey structure is slightly different from that of the 24-storey structure, and because higher structural vibration modes also contribute to the responses.

The above observations indicate that for high-rise adjacent structures, relative displacement is mainly caused by their different vibration properties if their vibration periods differ noticeably. When adjacent structures have similar vibration characteristics, however, relative displacement is mainly induced by ground motion spatial variations. Ground motion spatial variation effect is most significant when the phase shift between ground motions at outermost supports of two adjacent structures is out-of-phase with structural vibration mode. Neglecting ground motion spatial variations could underestimate relative displacement between adjacent structures by about 50 per cent if two adjacent high-rise structures have similar vibration properties. The spatial ground motion phase shift effect is more important than the coherency loss effect to high-rise structures and coherency loss effect generally could be neglected.

It is known that ground motion phase shift effect is more important to flexible structures while coherency loss effect is more significant to stiff structures.¹⁴⁻¹⁶ To study the spatial ground motion effect on low-rise stiff structures, relative displacement between the two 2-storey structures are calculated. Figure 7 shows the results obtained with different f_p and by continuously varying the mass of one structure. As can be seen, reducing f_p results in larger relative

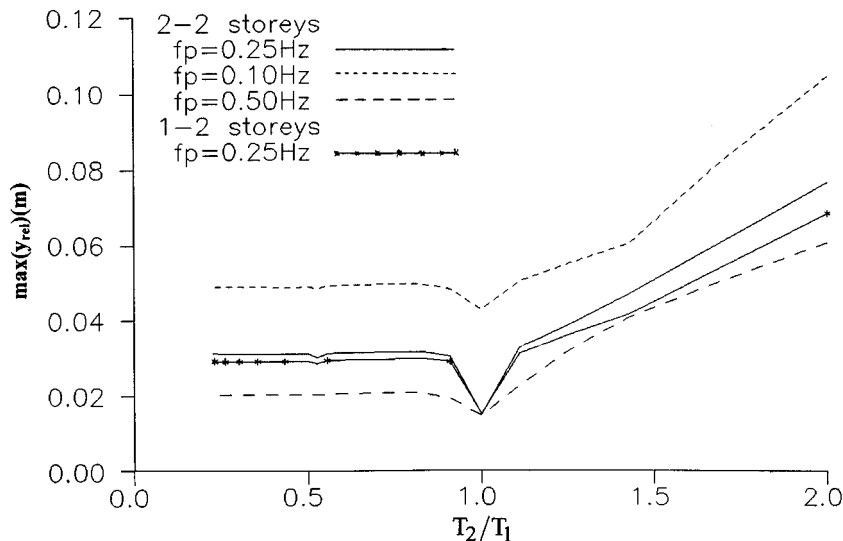


Figure 7. Peak relative displacement calculated with different central frequencies of high pass filter f_p

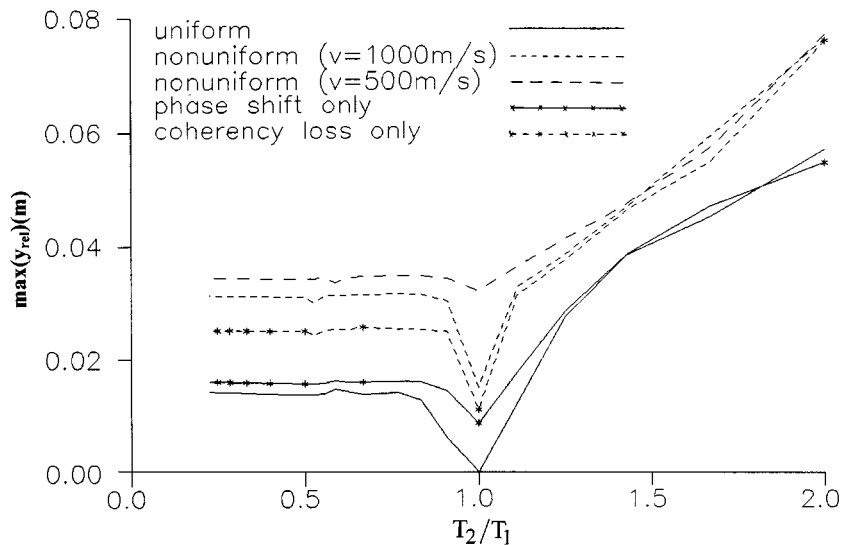


Figure 8. Peak relative displacement calculated with different ground motion spatial variations

displacements. This observation indicates that relative displacement depends strongly on quasi-static response as it is sensitive to the value of f_p , which in turn affects ground displacement significantly.

Using $f_p = 0.25$ Hz, and continuously varying the mass of the 1-storey structure, relative displacement between the 1- and the 2-storey structures is calculated and results are also shown in Figure 7. As can be seen, when the two buildings have different vibration periods the relative displacement is smaller than that between the two 2-storey structures. As the vibration period ratio increases, the difference between the relative displacements of 2–2 storey buildings and 1–2 storey buildings becomes more and more pronounced because of the increase in dynamic responses. It, however, remains a constant when $T_2/T_1 < 1.0$ because of the domination of quasi-static responses which are independent of structural vibration periods.

Figure 8 shows the relative displacement between the two 2-storey structures obtained by using multiple excitations with different spatial variations. When T_2 is less than T_1 , relative displacement is almost a constant for each input case, implying the domination of ground motion spatial variation effect (primarily coherency loss effect). When T_2 is larger than T_1 , ground motion spatial variation effect is still very pronounced, but the effect of different structural vibration properties of adjacent structures becomes more and more significant. Unlike high-rise structures, to which ground motion phase shift effect is more important, coherency loss effect is more significant to low-rise structures. This is because the coherency loss effect is more important to quasi-static responses while the phase shift effect is more important to dynamic responses.^{14–16}

The importance of coherency loss effect on low-rise structures can be further observed in Figure 9, where relative displacement between the 1- and the 2-storey structures ($T_2/T_1 = 1.25$) is shown with respect to the dimensionless parameter $f d/v$, in which f is natural frequency of the 2-storey structure. As can be seen, relative displacement corresponding to the nonuniform excitations increases with $f d/v$ without oscillating. The numerical values are very close to the

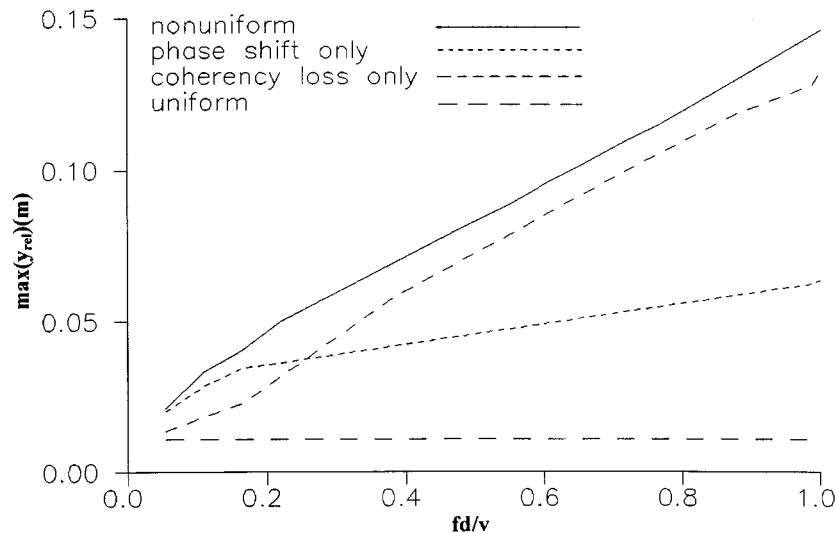


Figure 9. Peak relative displacement between 1- and 2-storey structures obtained with different span lengths and ground motion spatial variations

quasi-static relative displacement as shown in Figure 3. This observation indicates that the relative displacement consists mainly of quasi-static relative displacement and dynamic relative displacement, which oscillates with fd/v , is negligible. This is because of the dynamic deamplification effect caused by the much higher natural frequencies of two low-rise structures than the dominant ground motion frequencies.

It should be noted that the above numerical results are valid to shear-beam-type buildings with two column lines only. For buildings with more than two columns, the spatial ground motion phase shift effect will be less significant due to the averaging of the wave passage effect by columns. The coherency loss effect, however, will be the same. The above numerical results also indicate that the code specifications based on the dynamic responses of adjacent buildings might overestimate the required separations between adjacent high-rise structures since they neglect response phase difference. On the other hand, they might underestimate the relative displacement between low-rise adjacent buildings because they neglect spatial ground motion induced quasi-static responses.

CONCLUSIONS

Random vibration method has been employed to study the relative responses between adjacent building structures. The effects of ground motion spatial variations and structural vibration characteristics on relative displacement are investigated. Maximum relative displacements between realistic RC high-rise and low-rise structures have been calculated. It has been found that out-of-phase vibrations caused by different vibration periods are mainly responsible for relative displacement of adjacent high-rise structures. Ground motion spatial variation effect is only important to adjacent high-rise structures with close vibration periods. On the other hand, the

spatial ground motion effect is more significant on low-rise structures. For 1- or 2-storey structures, the relative displacement consists of primarily quasi-static relative displacement induced by nonuniform ground motions. Neglecting ground motion spatial variations greatly underestimates relative displacement between low-rise structures. Spatial ground motion phase shift effect is usually more important than its coherency loss effect to high-rise structures, while coherency loss effect is generally more important to low-rise structures.

APPENDIX

For a zero mean stationary process $x(t)$ with a power spectral density function $S(\bar{\omega})$, its m th-order spectral moment can be approximately estimated by

$$\lambda_m \approx \int_0^{\omega_c} \bar{\omega}^m S(\bar{\omega}) d\bar{\omega} \quad (28)$$

where ω_c is a high cut-off frequency.

The zero mean cross rate ν and the shape factor of the power spectral density function δ can be obtained by

$$\nu = \frac{1}{\pi} \sqrt{\frac{\lambda_2}{\lambda_0}} \quad (29)$$

$$\delta = \sqrt{1 - \frac{\lambda_1^2}{\lambda_0 \lambda_2}} \quad (30)$$

The mean peak response can then be calculated by²⁸

$$x_{\max} = \left(\sqrt{2 \ln \nu_e T} + \frac{0.5772}{\sqrt{2 \ln \nu_e T}} \right) \sigma \quad (31)$$

where T is duration of the stationary process, $\sigma = \sqrt{\lambda_0}$ is the standard deviation of the process, and

$$\nu_e T = \begin{cases} \max(2.1, 2\delta T), & 0 \leq \delta < 0.1 \\ (1.63\delta^{0.45} - 0.38)\nu T, & 0.1 \leq \delta < 0.69 \\ \nu T, & \delta \geq 0.69 \end{cases} \quad (32)$$

In this study, $T = 20$ s and a high cut-off frequency of $\omega_c = 25$ Hz, which covers the dominant ground excitation and primary structural vibration frequencies, are used.

REFERENCES

1. E. Rosenblueth and R. Meli, 'The 1985 earthquake: cause and effects in Mexico City', *Concrete Int. ACI* **8**(5), 23–24 (1986).
2. S. A. Anagnostopoulos, 'Building pounding re-examined: how serious a problem is it? Paper No. 2108', *Proc. 11th WCEE*, Acapulco, Mexico, 23–28 June 1996.
3. K. Kasai and B. F. Maison, 'Observation of structural pounding damage from the 1989 Loma Prieta earthquake', *Proc. 6th Canadian Conf. on Earthquake Engineering*, Toronto, 1991, pp. 735–742.

4. S. A. Anagnostopoulos, 'Earthquake induced pounding: state of the art', *Proc. 10th European Conf. on Earthquake Engineering*, Vienna, Austria, Vol. 2, 1995, pp. 897–905.
5. A. Wada, Y. Shinozaki and N. Nakamura, 'Collapse of building with expansion joints through collision caused by earthquake motion', *Proc. 8th World Conf. on Earthquake Engineering*, San Francisco, California, Vol. 4, 1984, pp. 855–862.
6. S. A. Anagnostopoulos, 'Pounding of buildings in series during earthquakes', *J. Earthquake Engng. Struct. Dyn.* **16**, 443–456 (1988).
7. B. F. Maison and K. Kasai, 'Analysis for the type of structural pounding', *J. Struct. Engng. ASCE* **116**(4), 957–977 (1990).
8. M. Papadrakakis and H. Mouzakis, 'Earthquake simulator testing of pounding between adjacent buildings', *J. Earthquake Engng. Struct. Dyn.* **24**, 811–834 (1995).
9. A. Filiatrault, M. Cervantes, B. Folz and H. Prion, 'Pounding of buildings during earthquakes: a Canadian perspective', *Can. J. Civil Engng.* **21**, 251–256 (1994).
10. E. Leibovich, A. Rutenberg and D. I. Yankelevsky, 'On eccentric seismic pounding of symmetric buildings', *J. Earthquake Engng. Struct. Dyn.* **25**, 219–233 (1996).
11. *Int. Conf. of Building Officials*, 'Uniform building code (UBC)', Whittier, California, U.S.A., 1993.
12. National Research Council of Canada, 'National building code of Canada (NBCC)', Ottawa, Ontario, Canada, 1990.
13. Chinese Academy of Building Research, 'Seismic design code for building and structures - GBJ11-89', Beijing, China, 1989 (in Chinese).
14. H. Hao, 'Arch responses to correlated multiple excitations', *J. Earthquake Engng. Struct. Dyn.* **22**, 389–404 (1993).
15. R. Harichandran and W. Wang, 'Response of indeterminate two-span beam to spatially varying seismic excitation', *J. Earthquake Engng. Struct. Dyn.* **19**, 173–187 (1990).
16. A. Zerva, 'Response of multi-span beams to spatially incoherent seismic ground motions', *J. Earthquake Engng. Struct. Dyn.* **19**, 819–832 (1990).
17. H. A. Jing and M. H. Young, 'Impact interactions between two vibration systems under random excitation', *J. Earthquake Engng. Struct. Dyn.* **20**, 667–681 (1991).
18. V. Jeng, K. Kasai and B. F. Maison, 'A spectral difference method to estimate building separation to avoid pounding', *Earthquake Spectra* **8**(2), 201–203 (1992).
19. V. Jeng and K. Kasai, 'Spectral relative motion of two structures due to seismic travel waves', *J. Struct. Engng. ASCE* **122**(10), 1128–1135 (1996).
20. K. Kasai, R. A. Jagiasi and V. Jeng, 'Inelastic vibration phase theory for seismic pounding mitigation', *J. Struct. Engng. ASCE* **122**(10), 1136–1146 (1996).
21. J. Penzien, 'Evaluation of building separation distance required to prevent pounding during strong earthquakes', *J. Earthquake Engng. Struct. Dyn.* **26**, 849–858 (1997).
22. H. Tajimi, 'A statistical method of determining the maximum response of a building structure during an earthquake', *Proc. 2nd World Conf. on Earthquake Engineering*, Tokyo, Japan, Vol. 2, 1960, pp. 781–797.
23. J. H. Lin, 'Separation distance to avoid seismic pounding of adjacent buildings' *J. Earthquake Engng. Struct. Dyn.* **26**, 395–403 (1997).
24. R. Ruiz and J. Penzien, 'Probabilistic study of the behaviour of structures during earthquake', *Report No. UCB/EERC 69-03*, Earthquake Engineering Research Center, University of California at Berkeley, California, 1969.
25. H. Hao, 'Effects of spatial variation of ground motions on large multiply-supported structures', *Report No. UCB/EERC-89/06*, Earthquake Engineering Research Center, University of California at Berkeley, Berkeley, California 94720, 1989.
26. H. Hao, 'Parametric study of the required seating length for bridge deck during earthquake', *J. Earthquake Engng. Struct. Dyn.* **27**, 91–103 (1998).
27. E. L. Wilson, 'CAL-91 - Computer assisted learning of structural analysis', *Report No. UCB/SEMM-91/01*, Department of Civil Engineering, University of California at Berkeley, 1991.
28. A. Der Kiureghian, 'Structural response to stationary excitation', *J. Engng. Mech. ASCE* **106**(6), 1195–1213 (1980).